Surface Reconstruction with Triangular Bézier Patches from Range Measurements

Patrick Chouraqui, Gershon Elber
Dept. of Computer Science
Technion, Israel Inst. of Technology
Haifa 32000, Israel

Eyal Zussman
Dept. of Mechanical Engineering
Technion, Israel Inst. of Technology
Haifa 32000, Israel

October 14, 1999

Abstract

Freeform surfaces can be described as a set of parametric triangular patches whose boundaries are linked one to another. This paper proposes a surface reconstruction method that is based on this fact. A set of range laser measurements are taken so that they define triangularly-bounded domains on the measured artifact, exploiting the spatial coherence in the measurements. Each bounded domain is filled with a triangular Bézier patch and the resulting surface is constrained to be G^1 continuous.

Using this approach, we have successfully captured the geometry of a variety of objects.

Keywords: Reverse Engineering, Triangular Gregory Patches, Triangular Bézier Patches, Range Laser.

1 Introduction

The motion picture industry must often create synthetic characters or objects. A common practice nowadays to digitally construct such objects is to start from a clay model and then digitize it. The surface geometry is then reconstructed from this set of digitized measurements.

There are typically two types of digitized data (input to the reconstruction process): an unorganized set of points, which is also denoted as a cloud of points, or a set of points with a specific geometric configuration.

An ordered set of points can typically be obtained by using a laser scanner (a range sensor). This set can be rearranged into a set of planar piecewise linear curves (or planar polylines). In this study, we have developed a method for reconstructing a surface while exploiting the coherency in the data acquired by the laser scanner.

Using a set of laser measurements, [Choi95] defines a Zmap structure: a uniform two dimensional grid containing the scanned depth value of the object for each (x, y) point. While this structure is useful for CSG operations, a real three dimensional object cannot be entirely described using Zmaps. Furthermore, this representation is discrete.

[Turk94] creates a polygonal representation of the measured object by progressively triangulating the areas between two consecutive parallel measurements.

[Deli94] uses a physical model to fit a simplex mesh upon a cloud of scanned points. Initially, a grid of particles (the simplex mesh) surrounds the set of scanned points. The particle system is then subjected to a set of forces so that the resulting mesh approximates the scanned surface after relaxation of the system.

Simple primitives such as spheres and cylinders are used in [Milr96] to approximate a set of points. Each primitive is fitted to a subset, M, of the initial set of points using a maximum likelihood algorithm. This algorithm estimates the parameters of the primitive that most probably corresponds to the set of approximated points, M.

In order to gain more accuracy in the final surface, it is useful to consider higher order surfaces. [Chen94, Krut95, Lai96, Seil96] tried to represent the reconstructed surface using a single Bspline patch. All these fitting methods are based on a least squares algorithm. [Chen94, Krut95] globally approximate the surface, while [Lai96, Seil96] make a two-phased approximation: First, coplanar points are approximated into a curve. Then, a surface approximation is created with curve sweeping.

In order to acquire the fine details of complex objects, [Eck96, Kris96] use a hierarchy of Bspline surfaces. [Eck96] first approximates the surface with a triangulation, and then rebuilds a set of rectangular domains on this triangulation that he finally fills with tensor product Bspline surfaces. [Kris96] defines regions on the scanned surface that are to be approximated with tensor product Bspline surfaces. Next, displacement maps are defined, which are three dimensional vector grids capable of capturing the fine details of the scanned surface.

[Hopp92, Hopp94a, Hopp94b] define a signed geometric distance function to the surface, S, that is to be reconstructed. The zero set of this function is approximated into a polygonal mesh, H_Z. Then, the number of faces in H_Z's is reduced by applying to H_Z a set of operations, such as edge-collapse, edge-split or edge-swap. Finally, a piecewise smooth subdivision surface is recursively created from the optimized mesh. A subdivision surface is defined by repeatedly refining the control mesh. In this case, the control mesh is composed of triangles. Consider a triangular face F on this mesh at phase i of the subdivision. Then, at phase $i+1$, F is replaced by four new triangular faces derived from F and its neighbors in the mesh.

[Pfei95, Pfei96] aim at building a DMS Spline Surface from scanned data. The DMS Spline surface is an extension of Bspline curves to the surface case, and can represent a polynomial surface upon a polygonal domain (not necessarily rectangular). First, the domain of the surface is triangulated and populated with DMS based functions $\{f_i\}$ (See [Pfei95] for further presentation of the DMS Spline surfaces). Then, a DMS Spline surface defined over

the base function $\{f_i\}$, is computed using a least squares approximation algorithm.

Rectangular patches are the most commonly used patches in geometric CAD applications. Nevertheless, triangular patches allow one to generate a greater panel of surfaces. [Baja92a, Baja94, Baja95, Bern96a] employ a set of algebraic triangular patches in modeling continuous surfaces. [Fari90] presents different kinds of triangular patches: triangular Bézier and Gregory patches, and studies their geometric properties.

In previous research, a geometric property of major concern was the continuity of the surface(s) approximating the scanned object. [Turk94] looks only at C^0 continuity in the reconstructed objects. In general, getting at least GC^1 smooth surfaces, also noted G^1 or geometrical continuity of order one, is a minimal practical requirement.

Bspline surfaces are C^{n-2} continuous when the order of the Bspline is n and no multiple knots are allowed. For example, an object approximated by a biquadratic Bspline surface is typically C^1. A Bézier surface is a single polynomial and hence is C^∞.

For an object to be approximated using a set of patches, the continuity between the patches must be studied and verified as well.

Given a global mesh, H, approximating the scanned surface (possibly obtained using a variant of [Hopp94b] method), [Eck96] builds a set of G^1 continuous Bspline tensor products over H, using the construction scheme of Peters [Eck96]. This construction scheme can be divided into two steps: given a closed mesh H, each face F of H is divided into a set of sub-meshes. For a given face F of H, a G^1 continuous set of Bézier tensor product surfaces is created on F. Finally, all the Bézier tensor product surfaces of a single face are unified into a single Bspline tensor product surface.

[Baja95] builds his A-patches so that each A-patch shares boundaries and normals on its boundary with its neighbors (sufficient conditions for getting G^1 continuity).

G^1 continuity between two adjacent triangular Bézier patches is addressed in [Fari90]. [Vata96] deals with continuity issues between different kind of patches: Bézier tensor product surfaces and triangular Gregory-Bézier patches in order to solve connection problems raised by generalized cylinders. A triangular bounded domain can be filled with either one triangular Gregory-Bézier patch, or, in order to increase control over the triangular domain, with three triangular Gregory-Bézier patches. In either case, the resulting surface is G^1 continuous at the patch boundaries. [Hage96] deals with G^2 continuity between triangular patches by considering both the tangent plane and the curvature at the patch boundaries.

1.1 Overview

Typical scanning operation involves a translational or rotational plane sweep, a plane that is the result of the laser's ray sweeping in space a plane. Hence, the result of the laser scan is a coplanar intersection curve between this plane and the visible (to the scanner) boundary of the object.

Let C_i and C_j be two different coplanar scanner's samples represented as two piecewise linear curves of m_i and m_j samples, respectively. A naive algorithm to find the intersection(s) between C_i and C_j would be in $O(m_i\ m_j)$ while one can exploit the computation complexity's plane sweep approach to yield an $O(m\ log\ m)$ algorithm with $m = \max(m_i,\ m_k)$. Nevertheless, and exploiting the spatial coherence of the scanners' output:

Lemma 1.1 *The k intersections between C_i and C_j can be computed in $O(k \log k\ m) = O(k \log k\ \max(m_i, m_j))$.*

Proof: Let $\mathcal{P}_i$ and $\mathcal{P}_j$ be the planes containing C_i and C_j. Further, let $\mathcal{L} = \mathcal{P}_i \bigcap \mathcal{P}_j$ be their intersection line. The k intersections of C_i and C_j must be on $\mathcal{L}$. Hence, find the segments in C_i (respectively C_j) that intersect $\mathcal{L}$, a computation that can be clearly conducted in $\mathrm{O}(m_i)$ (respectively $\mathrm{O}(m_j)$) time. having the k intersections in $\mathcal{L}$ for both C_i and C_j, sort and compare the two lists in $\mathrm{O}(k \log k)$. ■

Clearly k is a very small number, typically one. Hence, in practice, one can find the intersections of two scanner's coplanar samples in $\mathrm{O}(m)$. In the ensuing discussion, we will heavily employ this intersections' capability. Assume that the scanned object is genus zero, Then, the topology of the scanned curves is isomorphic to the plane. Furthermore, even if the scanner object is genus one or above, the translational and/or rotational nature of the scanning process suggests that in many cases the topology of the scanned curves is planar. In this work, and based on these observations, we reconstruct the topology of the scanned curves as a planar graph.

In this study, we develop a way to reconstruct an existing three dimensional object using a range laser. This surface reconstruction mechanism can be divided into three phases: data acquisition, construction of a topology from the data, and construction of a G^1 smooth surface using a set of triangular Gregory-Bézier patches. Section 2 presents and describes the reconstruction process of the topology of the object. A way to create a skeleton of the reconstructed surface using a set of curves is presented. From this set of curves we will extract a set of simplices that will be fitted with triangular Bézier patches, completing the geometry reconstruction in Section 3. The continuity of this set of patches will also be studied in Section 3. Finally, results of this research will be presented in Section 4, and conclusion drawn in Section 5.

2 Construction of a Network of Curves

Given a freeform artifact, $\mathcal{O}$, a range scanner is capable of providing the front most intersection of $\mathcal{O}$ with a plane, $\mathcal{P}$, which is a piecewise linear curve along $\mathcal{P}$ on $\mathcal{O}$. Given a triangular grid of measurements, which is a set of measurements that defines a set of triangular bounded domains on $\mathcal{O}$, the set, $\mathcal{I}$, of all possible intersections between two non parallel measurements is computed.

For each intersection, the normal of the measured surface at this intersection is also evaluated and directed toward the 'outside' of the measured freeform surface, or toward the scanner.

Definition 2.1 *Let $I_i, I_j \in \mathcal{I}$ be two intersections. I_i and I_j are* neighbors *if exists a piecewise linear curve C_k (a laser measurement) so that:*

1. *$I_i,\ I_j \in C_k$*
2. *no other intersections $I_p \in C_k$ exist between I_i and I_j on C_k.*

Given intersection I_i, the neighborhood of I_i, denoted $\mathcal{N}(I_i)$, is the set of all the neighboring intersections of I_i. The number of neighbors of I_i is denoted $||\mathcal{N}(I_i)||$.

The normal, N_i, of the scanned object at intersection I_i, will be oriented toward the scanner, outside from the scanner object.

2.1 The Construction of the Topology Graph

The resulting set of intersections can be organized into a planar graph structure $\mathcal{GI}(\mathcal{I}, \mathcal{E})$, $\mathcal{I}$ being the set of vertices and $\mathcal{E}$ the set of edges. Then, $\mathcal{GI}$ undergoes the following operations:

- unification: all pair of neighbors I_i, I_j so that $d(I_i, I_j) < \varepsilon$, with ε a user defined tolerance, are unified into a single node in $\mathcal{GI}(\mathcal{I}, \mathcal{E})$.
- consistency check: all nodes of $\mathcal{GI}$ connected to only one neighbor are removed from $\mathcal{GI}$.
- orientation: given $I_i \in \mathcal{GI}$, the set of the neighbors of I_i are angularly ordered according to a clockwise order as viewed along the normal direction, N_i

Definition 2.2 *Given I_i, $I_j \in \mathcal{GI}$ such that I_j is a neighbor of I_i, we denote by $next(I_i, I_j)$ the neighbor of I_j that follows I_i in the clockwise ordered list of neighbors of I_j, as viewed along N_i.*

2.2 Closed Loop of Curves (CLoC)

Definition 2.3 *Let $\mathcal{GI}$ be a planar graph of intersections, then a Closed Loop of Curves (CLoC) on $\mathcal{GI}$, $\{I_i\}_{i=1}^n$, is an ordered list of nodes so that:*

1. $1 < \forall i < n,\ I_{i+1} \in \mathcal{N}(I_i)$.
2. $I_1 \in \mathcal{N}(I_n)$.
3. $1 \leq \forall i, j \leq n,\ i \neq j \ \Rightarrow\ I_i \neq I_j$.

Definition 2.4 *Let $\{I_i\}_{i=1}^n$ be a CLoC on $\mathcal{GI}$. Then, $\{I_i\}_{i=1}^n$ is a minimal CLoC iff $\forall i > 1,\ I_{i+1} = next(I_{i-1}, I_i)$ mod n.*

By mod n we also assume in Definition 2.4 that $I_1 = next(I_{n-1},\ I_n)$ and $I_2 = next(I_n,\ I_1)$. This mod based computation will be hereafter implicitly assumed.

Given a planar graph of intersection, $\mathcal{GI}$, one compute the set of all the minimal CLoC of $\mathcal{GI}$ following the algorithm portrayed in Figure 1.

In the graph defined in the algorithm of Figure 1, all the edges are oriented. Initially, every edge in $\mathcal{GI}$ is thus represented as two directed edges in the opposite directions. Function `MarkOrientedEdge` marks the oriented edge as already used by a CLoC in the graph $\mathcal{GI}$. Boolean function `IsFreeOrientedEdge` returns `TRUE` only if the edge is not marked in the graph $\mathcal{GI}$.

```
BuildMinimalCLoC(I_i, I_j)
    FirstNode ⇐ I_i;
    While ((I_next = next(I_i, I_j)) ∉ CurrentCLoC and
            IsFreeOrientedEdge(I_j, I_next)) do
        begin
            I_i ⇐ I_j;
            I_j = I_next;
            MarkOrientedEdge(I_j, I_next);
            AddToCurrentCLoC(I_j);
        end
```

Figure 1: Building a minimal Closed Loop of Curves (CLoC).

2.3 Closed Loop of Bézier Curves (CloB)

Given a minimal CLoC $\{I_i\}_{i=1}^n$ in $\mathcal{GI}$, a set of Bézier curves fitting the CLoC $\{I_i\}_{i=1}^n$ is computed as follows: $1 \leq \forall i \leq n$, such that $I_i,\ I_{i+1} \in C_j$, a piecewise linear scanner's sample, the set of points of C_j between I_i and I_{i+1}, is approximated by a cubic Bézier curve $B_i(t) = \sum_{i=0}^3 Q_i \theta_i(t)$, where $\theta_i(t)$ are the Bézier basis function. $Q_0 = I_i$ and $Q_3 = I_{i+1}$ due to positional end condition. The location of the two inner control points of $B_i(t)$ is determined using a least-squares fit to the rest of the points in C_j.

3 Triangular Bézier and Gregory Patches

In this section, the following notations will be employed:

$$\binom{n}{i} = \frac{n!}{i!(n-i)!}, \qquad \binom{n}{i\ j} = \frac{n!}{i!j!(n-i-j)!}.$$

Also denote by $\mathcal{K}$ the set $\mathcal{K} = \{(i,j,k) \in [0,n]^3 \mid i+j+k = n\}$. Furthermore, throughout this section, the following relations of $u+v+w=1$ and of $i+j+k=n$ will always hold. With that, the following shortening notation will also be exploited:

$$\begin{aligned} P_{ij} &= P_{ijk}, \\ P_{ij}(u,v) &= P_{ijk}(u,v,w), \\ \theta_{ij}^n(u,v) &= \theta_{ijk}^n(u,v,w), \\ S(u,v) &= S(u,v,w), \end{aligned}$$

where $P_{ijk}(u,v,w)$, $\theta_{ijk}^n(u,v,w)$, and $S(u,v,w)$ are functions of the parameters (u,v,w), such that $u+v+w=1$.

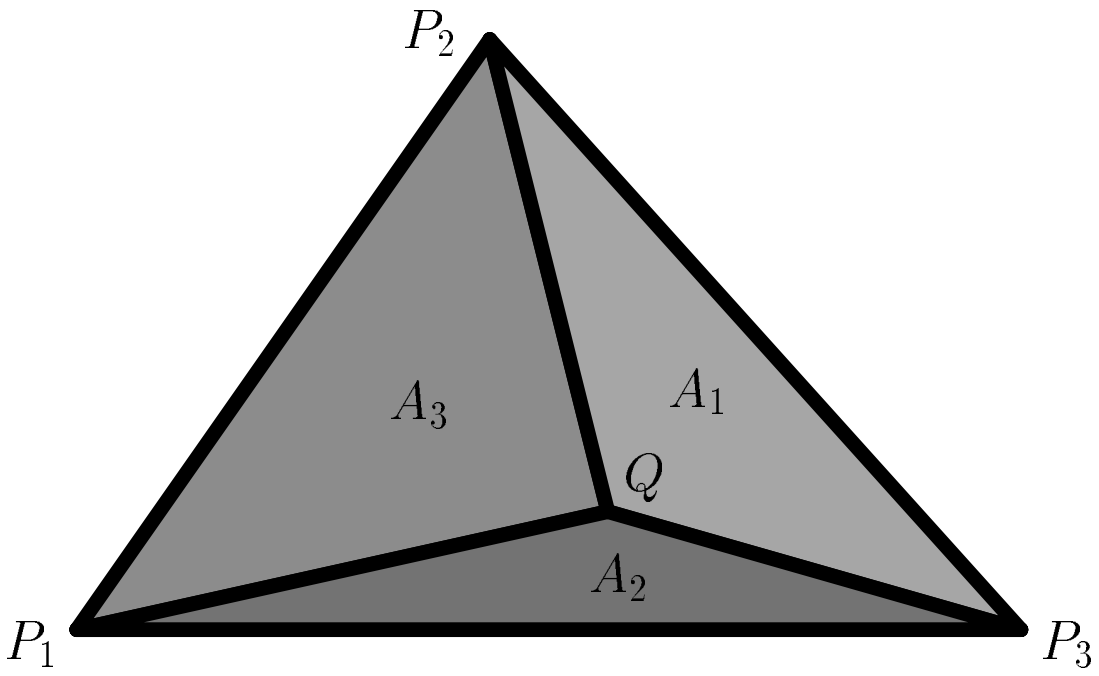

Figure 2: Given triangle T, the barycentric coordinates of point Q with respect to the vertices of T are computed based on the rations of the areas of the three triangles A_i, $i = 1, 2, 3$.

3.1 Triangular Bézier Patch

Let T be a triangle with vertices P_i, $i = 1, 2, 3$ (See Figure 2), and let Q be a point in T. Then, let $(u, v, w) \in \mathbb{R}^3$ be such that $Q = uP_1 + vP_2 + wP_3$.

Define the three sub-triangles T_1, T_2 and T_3 so that each triangle is composed of two vertices of T and the point Q. Then, we have the following geometrical properties:

$$u = \frac{A_1}{A}, \qquad v = \frac{A_2}{A}, \qquad w = \frac{A_3}{A},$$

where $A = Area(T)$ and $A_i = Area(T_i)$. (u, v, w) are call the *barycentric* coordinate of point Q with respect to P_i, $i = 1, 2, 3$.

Let $\{P_{ijk}\}_{(i,j,k)\in\mathcal{K}} \in \mathbb{R}^3$ be three dimensional points, u, v and w be the barycentric coordinates of some point Q in the triangular parameter domain, $u + v + w = \frac{A_1}{A} + \frac{A_2}{A} + \frac{A_3}{A} = 1$. Then, a triangular Bézier patch of degree n is defined by (See Figure 3):

$$S(u, v, w) = \sum_{i=0}^{n} \sum^{n-i} P_{ijk}\theta^n_{ijk}(u, v, w),$$

where $\theta^n_{ijk}(u, v, w)$ is the generalized Bernstein Bézier polynomial of degree n defined as:

$$\theta^n_{i,j,k}(u, v, w) = \frac{n!}{i!j!k!}u^i v^j w^k = \binom{n}{i\ j} u^i v^j (1 - u - v)^{n-i-j} = \theta^n_{ij}(u, v).$$

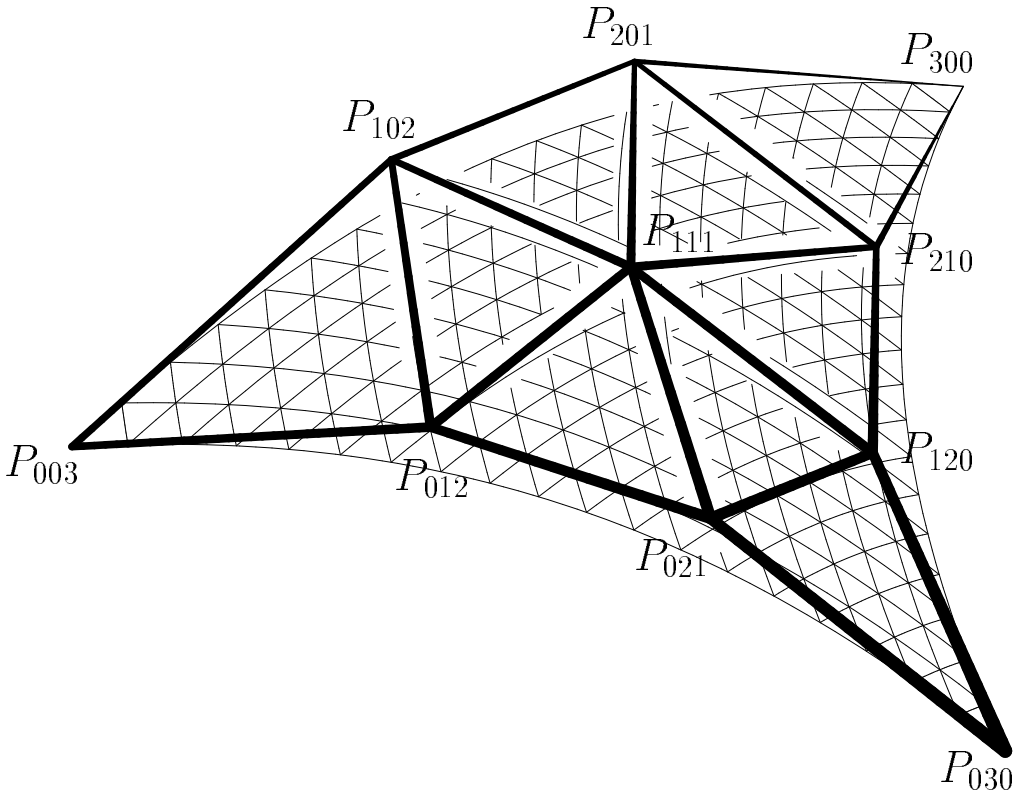

Figure 3: A triangular parametric cubic Bézier Patch.

3.2 G^1 Continuity Along a Common Boundary

Definition 3.1 *Two adjacent triangular Bézier patches are G^1 continuous iff*

1. *The two patches are C^0 continuous, that is, they share a common boundary curve C_b.*
2. *Along their shared boundary curve, C_b, the tangent plane is identical on both sides of C_b.*

Two different approaches to achieving G^1 continuity between adjacent triangular Bézier patches can be attempted:

1. Consider the continuity constraint as a global problem, and resolve it globally for all patches simultaneously.
2. Coerce each triangular Bézier patch to follow a predetermined tangent plane on its boundaries. Thus, for a given shared boundary curve, the tangent planes in both sides of every given point on the boundary curve will be identical. In this case, the continuity problem can be locally treated on each individual triangular Bézier patch.

Clearly, the second alternative is more numerically robust, and efficient to compute while it might be non optimal. It is this second approach that we have chosen to employ as part of this work.

3.3 The Limitations of Triangular Bézier Patches

In order to achieve G^1 continuity, one needs to impose constraints on the tangent planes at all three boundary curves of each triangular Bézier patch. For each boundary point, the tangent plane can be determined by the tangent field of the boundary curve at this point, and the cross derivative of the patch in some other direction. Hence, the tangent plane along each boundary depends on the control points that define the boundary curve, and on one internal row of control points next to it, that completely prescribes the boundaries' cross derivative.

Yet, continuity must be achieved on all three sides of the triangular patch. As a result, one is faced with three different G^1 continuity constraints that need to be resolved. These three G^1 continuity problems are not *independent*, because of shared variables that are over-constrained at the three corners of the patch. For a cubic triangular patch (See Figure 3), the central control points, $P_{1,1}$ is over-constrained from all three boundaries. For a higher order triangular patch, the three interior control points $P_{1,1}$, $P_{1,n-2}$, and $P_{n-2,1}$ are prescribed and constrained from two different boundaries. Both cases result in an inability to resolve the G^1 continuity problem, in general. In order to simplify the G^1 constraints problem, we will decouple the problem at each boundary of the triangle from the other two. Toward this end, we will exploit the triangular Gregory patch, an extension of the triangular Bézier patch that will be considered in the next section.

3.4 Triangular Gregory Patches

Let $\{P_{ijk}\}_{(i,j,k)\in\mathcal{K}} \in \mathbb{R}^3$ be a set of three dimensional points and let $P_{ijk}(u,v,w) : [0,1]^3 \rightarrow \mathbb{R}^3$ be trivariate functions in $\mathbb{R}^3$ with parameters (u,v,w) that satisfy $u+v+w=1$. Further, let $\{P^u_{ijk},\ P^v_{ijk},\ P^w_{ijk}\}$ be a decomposition of point P_{ijk} into:

for $(n=3)$:

$$P_{ijk}(u,v,w) = \begin{cases} \frac{vwP^u_{111}+uwP^v_{111}+uvP^w_{111}}{vw+uw+uv} & \text{if } (i,j,k)=(1,1,1), \\ P_{ijk} & \text{otherwise.} \end{cases}$$

for $(n>3)$:

$$P_{ijk}(u,v,w) = \begin{cases} \frac{(1-v)uP^u_{1,1,n-2}+(1-u)vP^v_{1,1,n-2}}{(1-v)u+(1-u)v} & \text{if } (i,j,k)=(1,1,n-2), \\ \frac{(1-w)vP^v_{1,n-2,1}+(1-v)wP^w_{1,n-2,1}}{(1-w)v+(1-v)w} & \text{if } (i,j,k)=(1,n-2,1), \\ \frac{(1-w)uP^u_{n-2,1,1}+(1-u)wP^w_{n-2,1,1}}{(1-w)u+(1-u)w} & \text{if } (i,j,k)=(n-2,1,1), \\ P_{ijk} & \text{otherwise.} \end{cases} \quad (1)$$

Then, a triangular Gregory patch of degree n is defined as:

$$S(u,v,w) = \sum_{i=0}^{n}\sum_{j=0}^{n-i} P_{ijk}(u,v,w)\theta^n_{ijk}(u,v,w), \quad (2)$$

where $\theta^n_{i,j,k}(u,v,w)$ is the generalized Bernstein Bézier polynomial of degree n, as defined in Section 3.1.

Let $\{I_i\}_{i=1}^3$ be a CLoB composed of three Bézier curves $\theta_1(u)$, $\theta_2(v)$, $\theta_3(w)$ of degree n. To build a G^1 triangular Gregory patch $S(u,v)$ from this CLoB, the following constraints will be imposed:

1. The three corners of the triangle are points I_1, I_2, I_3.

2. The boundary curves of $S(u,v)$ will follow the three Bézier curves $\theta_1(u)$, $\theta_2(v)$, $\theta_3(w)$. These constraints prescribe the tangent plane at the three corners of the triangle, and hence the three normals, N_i $i = 1, 2, 3$, at these corners.

3. The tangent planes along the three boundary curves of $S(u,v)$ will be derived from the tangent planes at the corners of the triangle. This constraint prescribes a normal vector field along the three boundaries. For a given boundary curve $\theta_1(u)$ between I_i and I_j, the normal of $S(u,v)$ at a given point along $\theta_1(u)$ will be some combination of N_i and N_j, the normals at I_i and I_j, a combination that will be described shortly.

Given two adjacent CLoBs $\{I_i\}_{i=1}^3$ and $\{I_i\}_{i=2}^4$, the resulting Gregory Patches $S_1(u,v)$ and $S_2(u,v)$ will be C^0 continuous since they share a common boundary curve, $\theta_1(u)$ between I_2 and I_3 (constraints 1 and 2). Moreover, at the corner of S_1 and S_2, on the common boundary curve, tangent planes will be the same. Then, the tangent plane at every point along C will be the same for both patches. That is, the patches S_1 and S_2 will be G^1 continuous.

Without loss of generality, consider the boundary curve $B_1(u) = S(u,0)$ between I_2 and I_3. The tangent plane along $B_1(u)$ will be defined with the aid of the following two vectors fields:

1. The tangent field of the surface S along the boundary curve, $T_1(u) = \frac{\partial B_1(u)}{\partial u}$.

2. A second vector field $R_1(u)$ that is defined as follows:
   Let $R_1(0) = N_1 \times T_1(0)$ and $R_1(1) = N_2 \times T_1(1)$. Then, $R_1(u) = uR_1(1) + (1-u)R_1(0)$.

Let $D_1(u) = \frac{\partial S(u,v)}{\partial v} \mid_{v=0}$ be a cross derivative of $S(u,v)$ along boundary curve $B_1(u)$. Provided S is regular, $(T_1(i), R_1(i))$, $i = 0, 1$ form a basis for the tangent plane at the corners. There exists a unique pair of scalar values (k_1, h_1) that satisfies: $D_1(0) = k_1 T_1(0) + h_1 R_1(0)$. Similarly, there exists a unique pair (k_2, h_2) that satisfies: $D_1(1) = k_2 T_1(1) + h_2 R_1(1)$.

Let $k(u) = uk_2 + (1-u)k_1$ and $h(u) = uh_2 + (1-u)h_1$ be two linear polynomial functions. Then,

$$D_1(u) = k(u)T_1(u) + h(u)R_1(u), \tag{3}$$

resulting in a vector field $D_1(u)$ that belongs to the constrained tangent plane of $S(u,v)$ along boundary curve $B_1(u)$. When fixing parameter u, $D_1(u)$ appears as a linear combination of at most $2n+1$ control points: the $n+1$ control points that define $B_1(u)$, the boundary curve, and n control points on the next internal row. On this $2n+1$ control points, $n+3$ are already defined by the boundary curves of the CLoB. By judiciously sampling Equation (3) at $(n-2)$ values of u, one gets a linear system of $(n-2)$ equations with $(n-2)$ unknowns (the internal control points). Thus, the resolution of this system will provide the internal row of control points of $S(u,v)$ adjacent to boundary curve $B_1(u)$.

A similar constraint to Equation (3) is solved for each of the three boundary curves of $S(u,v)$, in order to create a Gregory patch that is G^1 continuous with all its neighboring patches.

Let $B_1(u)$ be of degree n. Then, in Equation (3), $D_1(u)$ should be of degree n, and $S(u,v)$ should be of degree $n+1$.

A triangular parametric Bézier patch of degree n has $(n+1)(n+2)/2$ control points. For a degree four ($n=4$) patch, we have $15=(4+1)(5+1)/2$ control points. For a Gregory patch of degree four, one needs to resolve $18=15+3$ unknown control points, due to the three splitted points. The boundary curves prescribe the 12 external control points and the resolution of Equation (3) constrains two internal control points for each boundary curve.

For a Gregory patch of higher degree, more degrees of freedom are available that could possibly allow the user to satisfy additional physical constraints to the reconstructed surface, such as convexity.

3.5 From Gregory Patches to Rational Triangular Bézier Patches

Since the triangular Bézier patches have simple evaluation and display procedures, we seek methods to convert a triangular Gregory patch to a triangular Bézier patch. Previous work has been done to convert rectangular Gregory patches to Bézier patches (See [Taka90]). We have used their general scheme and extended it to triangular Gregory patches as well.

Consider Equation (2), the equation of a triangular Gregory patch of degree n, and let $X(u,v,w)=(u(1-v)+v(1-u))(v(1-w)+w(1-v))(w(1-u)+u(1-w))$ be the product of all possible denominators in $P_{ijk}(u,v,w)$, and is of degree six. Let $Q(u,v,w)=S(u,v,w)X(u,v,w)$, or $S(u,v,w)=\frac{Q(u,v,w)}{X(u,v,w)}$ where the degree of Q is $n+6$. Because $u+v+w=1$, one can easily raise the degree of polynomial X to $n+6$, by multiplying X by $(u+v+w)^n$.

Let $\mathbb{R}_{n+6}[X]$ (resp. $\mathbb{R}^3_{n+6}[X]$) be the vector space of trivariate polynomials of degree $n+6$ on $\mathbb{R}$ (resp. on $\mathbb{R}^3$). Then, $\{\theta^{n+6}_{ijk}(u,v,w)\}_{(i,j,k)}$ is a basis of $\mathbb{R}_{n+6}[X]$ (resp. of $\mathbb{R}^3_{n+6}[X]$) (See [Boeh93] for further discussion on Bernstein basis functions).

Thus, it is possible to find a unique decomposition of $X(u,v,w)$ using the basis function $\{\theta^{n+6}_{ijk}(u,v,w)\}_{(i,j,k)}$, as, $X(u,v,w)=\sum\sum w_{ijk}\theta^{n+6}_{ijk}(u,v,w)$, with $w_{ijk}\in\mathbb{R}$.

Similarly, it is possible to find a unique decomposition of $Q(u,v,w)$ using the basis function of $\{\theta^{n+6}_{ijk}(u,v,w)\}_{(i,j,k)}$ as, $Q(u,v,w)=\sum\sum Q_{ijk}\theta^{n+6}_{ijk}(u,v,w)$, with $Q_{ijk}\in\mathbb{R}^3$.

Let $\overline{Q_{ijk}}\in\mathbb{R}^3$ be such that $\overline{Q_{ijk}}=\frac{Q_{ijk}}{w_{ijk}}$. Then, one can write,

$$S(u,v,w)=\frac{Q(u,v,w)}{X(u,v,w)}=\frac{\sum\sum w_{ijk}\overline{Q_{ijk}}B^{n+6}_{ijk}(u,v,w)}{\sum\sum w_{ijk}B^{n+6}_{ijk}(u,v,w)},$$

which is the equation of the rational parametric triangular Bézier patch of degree $n+6$.

4 Result and Examples

The method presented here proposes a way to produce a smooth surface from a reduced number of measurements, using the unique geometric properties of laser scanner measure-

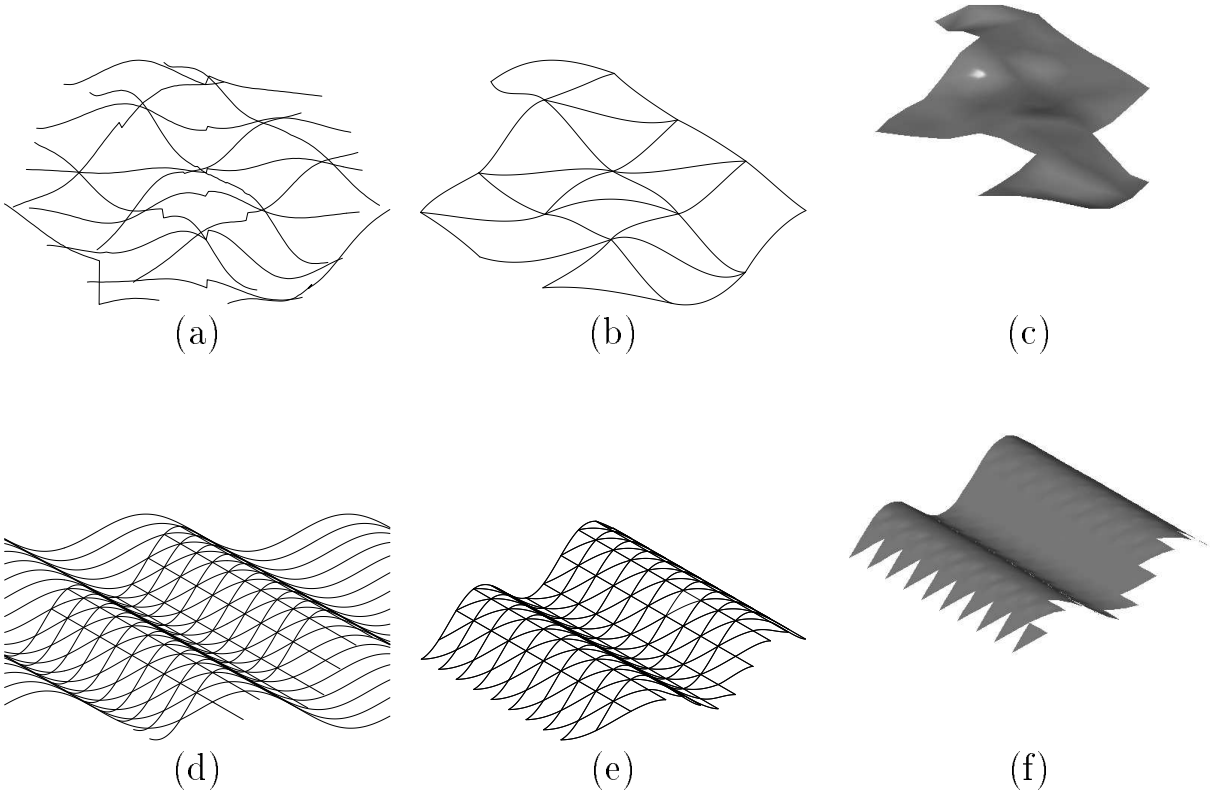

Figure 4: (a) shows noisy scanner measurements of a freeform surface. (d) shows an artificial surface. (b) and (e) show the set of minimal CLoBs generated from (a) and (d). Finally, (c) and (f) show the triangular Bézier patches generated from the measurements, (a) and (d).

ments, and the coherence in its samples. In all presented examples, the triangular Gregory patches are converted to triangular Bézier patches for display purposes.

Figure 4 presents some simple examples. In Figures 4 (a) and (d) the scanner's data is presented. Figure 4 (b) and (e) shows the reconstructed topology as minima CLOBs, whereas Figures 4 (c) and (f) portrays the final reconstructed geometry. Note that the geometry, in the form of triangular parametric Gregory patches, is fitted only to triangular CLoBs.

Figure 5 presents a more realistic example of a face reconstruction. As presented in the figure, the more measurements, the better is the level of accuracy that can be achieved, for the measured artifact. The reconstruction using the approach presented in this work (in Figures 5 (c), (f), and (i)) is compare to a simple triangulation of the data (in Figures 5 (b), (e), and (h))

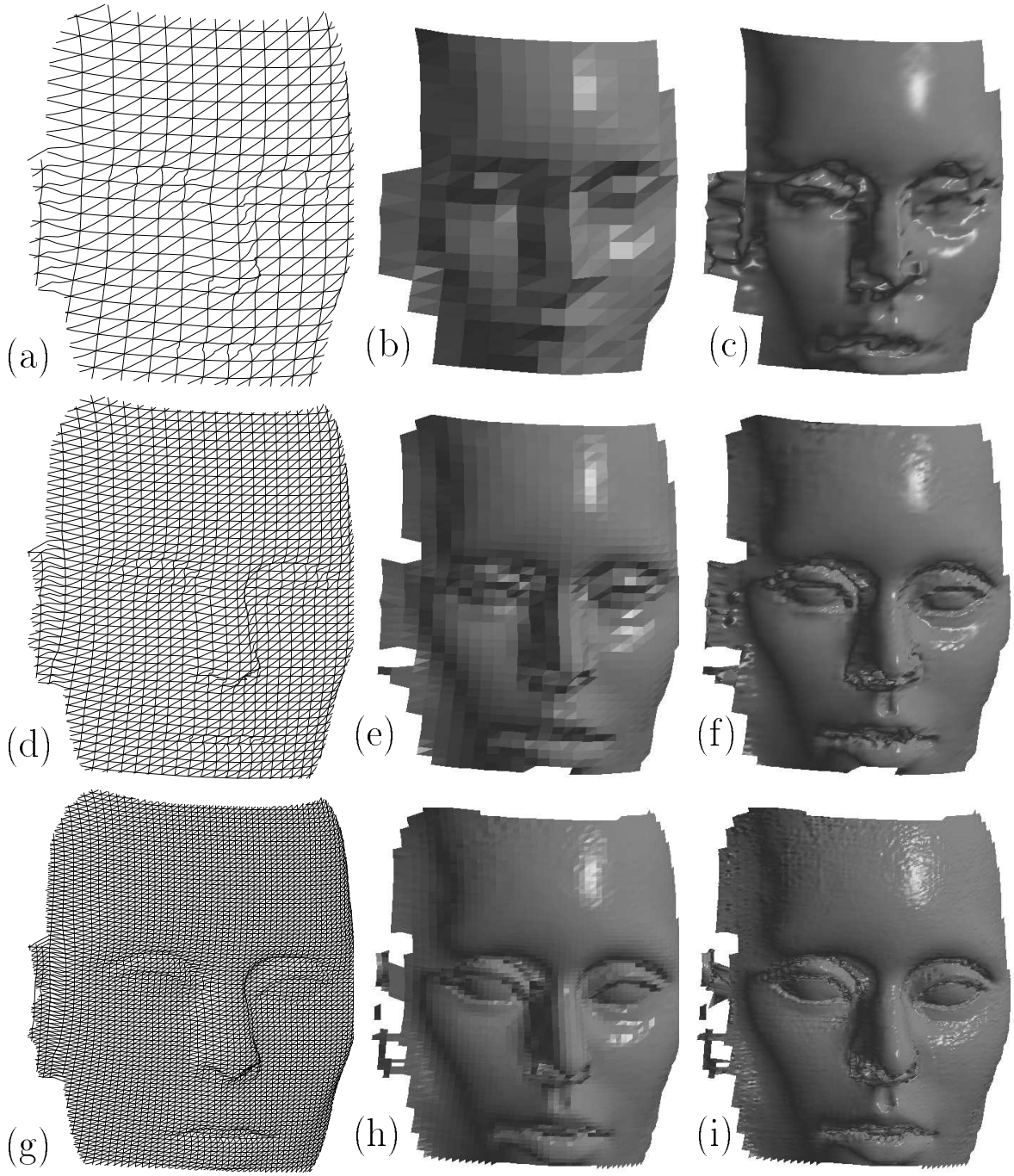

Figure 5: *From measurements in low (a), medium (d) and high (g) levels of accuracy, intersections are computed. In (b), (e) and (h), these sets of intersections are triangulated. In comparison, in (c), (f) and (i), the proposed algorithm is applied on the measurements of (a), (d) and (g).*

5 Conclusions and Future Work

We have presented a geometry reconstruction approach that employs triangular parametric patches. Nothing in the presented scheme prevents from using other types of triangular patches in the geometry reconstruction stages, patches such as the A-patches.

No error estimation over the reconstructed surface is conducted in this work. The obvious problem of lack of information in the interior of a minimal CLoC is a major hinder factor in any such attempt. Yet, the presented approach lend itself with ease to an *adaptive reconstruction.* Consider the forehead region, in Figure 5. The low resolution reconstruction, in Figure 5 (c) is sufficient. Yet, in other areas, such as the eyes and the mouth, a higher resolution reconstruction is necessary, as in Figure 5 (i). Because each triangular domain can be subdivided into four such domains, an adaptive approach is clearly feasible and should be investigated.

Another major difficulty in any reconstruction scheme is handling or segmenting tangent discontinuities or sharp features in the object. Having detected the sharp edges, the presented approach could be applied to the interior, continuous, regions.

References

[Baja92a] C.L. Bajaj. *Surface Fitting with implicit algebraic surface patches.* H. Hagen Editor, Topics in Surface Modeling, pp 23-52, SIAM Publications, 1992.

[Baja94] C.L. Bajaj, J. Chen, G. Xu. *Free Form Surface Design with A-Patches.* Graphics Interface '94, pp 174-181, 1994.

[Baja95] C.L. Bajaj, F. Bernardini, G. Xu. *Automatic Reconstruction of Surfaces and Scalar Fields from 3D Scans.* Siggraph 95, Computer Graphics Proceedings, pp 109-118, 1995.

[Beng97] W.C. Bengtson, A. Fallon, D. Cambridge, D. William, D. King. *Digitizing on a Shoestring.* Computer Graphics World, April 1997, pp 75-76.

[Bern96a] F. Bernardini, C.L. Bajaj, J. Chen, D.R. Schikore. *Automatic Reconstruction of 3D CAD Models from Digital Scans.* 1996.

[Boeh93] W. Boehm, H. Prautzsch. *Numerical Methods*, 1993, Edition AK Peters.

[Chen94] Y. Chen, G. Johnson, D. Simon. *Fast Complex Surface Inspection and Verification using Optical Laser Line Scanner.* Transactions of NAMRI/SME, 1994, Volume 22, pp 247-252.

[Choi95] B.K. Choi, Y.C. Chung, J.W. Park. *Application and Extension of Z-Map Model.* pp 363-382, Computer Graphics and Applications, Pacific Graphics'95, Editor Shin, Kunii.

[Deli94] H. Delingette. *Simplex Meshes: a General Representation for 3D Shape Reconstruction.* Rapport de Recherche n 2214-Mars 1994-INRIA Sophia Antipolis, France.

[Eck96] M. Eck, H. Hoppe. *Automatic Reconstruction of B-Spline Surfaces of Arbitrary Topological Type.* Siggraph 96, Computer Graphics.

[Fari90] G. Farin. *Curves and Surfaces for computer-aided geometric design: a practical guide.* Academic Press, London, 1990.

[Hage96] H. Hagen, G. Nielson, Y. Nakajima. *Surface design using triangular patches.* Computer Aided Geometric Design 13 (1996), pp 895-904.

[Hopp92] H. Hoppe, T. DeRose, T. Duchamp, J. McDonald, W. Stuetzle. *Surface Reconstruction from Unorganized Points.* Siggraph 92, Computer Graphics, July 1992, pp 71-88.

[Hopp94a] H. Hoppe. *Surface Reconstruction from Unorganized Points.* PhD thesis, university of Washington, USA, 1994.

[Hopp94b] H. Hoppe, T. DeRose, T. Duchamp, M. Halstead, H. Jin, J. McDonald, J.Schweitzer, W. Stuetzle. *Piecewise Smooth Surface Reconstruction.* Siggraph 94, Computer Graphics Proceedings, Annual Conference Series, pp 295-302.

[Kris96] V. Krishnamurthy, M. Levoy. *Fitting Smooth Surfaces to Dense Polygon Mesh.* Computer Graphics Proceedings, annual conference series, 1996.

[Krut95] W. Ma, J.P. Kruth. *Parameterization of randomly measured points for least squares fitting of B-Spline curves and surfaces.* Computer Aided Design, Volume 27, Number 9, 1995, pp 663-675.

[Lai96] J.Y. Lai, C.Y. Lin, C.S. Liou. *A Reverse Engineering Approach for Complex Shape Modeling.* Automation '96, Proceedings, Volume one, pp 231-238.

[Milr96] M.J. Milroy, D.J. Weir, C. Bradley, G.W. Vickers. *Reverse Engineering Employing a 3D Laser Scanner: A Case Study.* Advanced Manufacturing Technology, 1996, pp 111-121.

[Pfei95] R. Pfeifle, H.P. Seidel. *Fitting Triangular B-Splines to Functional Scattered Data.* Graphics Interface '95, pp 26-33, 1995.

[Pfei96] R. Pfeifle, H.P. Seidel. *Triangular B-Splines for Blending and Filling of Polygonal Holes.* Graphics Interface '96, pp 186-193, 1996.

[Seil96] A. Seiler, V. Balendran, K. Sivayoganathan, A. Sackfield. *Reverse Engineering from Uni-Directional CMM Scan Data.* Advanced Manufacturing Technology, 1996, pp 277-284.

[Taka90] T. Takamura, M. Ohta, H. Toriya, H. Chiyokura. *A Method to convert a Gregory Patch and a Rational Gregory Patch to a Rational Bézier Patch and Its applications.* Chua T.S., Kunii T. L. (ed.), CG International (CGI) 90, pp 543-562.

[Turk94] G. Turk, M. Levoy. *Zippered Polygon Meshes from Range Images.* Siggraph 94, Computer Graphics, Volume 22, pp 311-318.

[Vata96] G. Vatant, B. Peroche. *Connection Problems raised by generalized cylinders.* Theory and Practice of Geometric Modeling, 1996.